

The JERS-1 Amazon Multi-Season Mapping Study (JAMMS): Science Objectives and Implications for Future Missions

Anthony Freeman, Bruce Chapman, Paul Siqueira
Jet Propulsion Laboratory
California Institute of Technology
4800 Oak Grove Drive
Pasadena, California 91109

Tel: (818) 354 1887

Fax: (818) 393 5285

e-mail: tony.freeman@jpl.nasa.gov

Abstract

In late September 1995, the National Space Development Agency of Japan (NASDA) began a new phase of operations for the Japanese Earth Remote Sensing satellite (JERS-1) Synthetic Aperture Radar (SAR) - the Global Rain Forest Mapping (GRFM) project. The first rain forest area to be mapped was the Amazon Basin, between September and November of that year (the low flood season for much of the region), in support of the JERS-1 Amazon Multi-season Study (JAMMS), sponsored by NASA. This data acquisition was repeated six months later to acquire a second map of the Amazon, during the high flood season in May/June of 1996. The main objective of the JAMMS project was to generate a map of inundation over the Amazon basin by comparing data from the high- and low-flood seasons. Most of the data collected during these two phases of the JAMMS project, a total of ~5000 frames of data, was received and processed by the Alaska SAR Facility, then sent to JPL and NASDA for post-processing and analysis.

The quality of the data processed by ASF for the JAMMS project has proved to be exceptional. This paper is a summary of the JAMMS project, which has resulted in a scientific data set of very high value – a multi-season snapshot of one of the most difficult areas on Earth to monitor.

1. Introduction

The Amazon rain forest is a region of the earth that is undergoing rapid change. Man-made disturbance such as clear cutting for agriculture or mining is altering the rain forest ecosystem. For many parts of the rain forest, seasonal changes from the wet to the dry season are also significant and fundamental to understanding the regional ecology. Changes in the seasonal cycle of flooding and draining can cause significant alterations in the forest ecosystem.

Because much of the Amazon basin is regularly covered by thick clouds, optical and infrared coverage from the LANDSAT and SPOT satellites is sporadic. Imaging radar offers a much better potential for regular monitoring of changes in this region. In particular, the JERS-1 satellite carried an L-band HH SAR system which, via an on-board type recorder, could collect data from almost anywhere on the globe, at any time of year.

The JERS-1 satellite, which stopped operating in 1998, traveled in a 568 km altitude orbit with a payload that included an L-band, HH-polarized SAR with a nominal 21m X 21m resolution, which imaged at incidence angles between 30 and 36 degrees (EORC, 1995). The JERS-1 SAR was the first polar-orbiting imaging radar system capable of monitoring the whole of the Earth's land surface, because of its on-board tape recorder system. Further, because of the ability of imaging radar to see through clouds, and the sensitivity of L-Band backscatter measurements to different biomass levels and flooded forest conditions, the JERS-1 SAR was well-suited to multi-temporal studies of the Earth's land surface.

Unlike the European ERS-1 SAR, which was primarily designed for studying the world's ocean and ice-covered areas, the wavelength, polarization, incidence angle and sensor performance of the JERS-1 SAR was optimized for studies of vegetation cover on land (Yoneyama et al, 1989). A look at some examples of JERS-1 SAR images over forested areas verifies this: clear-cut areas, flooded forests, marshland and water channels can easily be separated visually. On closer inspection, it can also be seen that flood plain forest areas in JERS-1 images have a smoother image texture than forests on higher ground.

NASDA initiated the GRFM project in 1995 (Rosenqvist, 1996). The objective of this project was to use the JERS-1 SAR to map the world's tropical rain forest regions at high resolution. This project, lead by NASDA's Earth Observation Research Center (EORC), and with key participation by NASA's Jet Propulsion Laboratory (JPL), and the Space Applications Institute of the European Commission's Joint Research Center (JRC/SAI), assembled a team of invited scientists to evaluate, analyze, and use the data.

One of the products of this task is the mosaicked imagery. This imagery may be found at the following website :

<http://trfic.jpl.nasa.gov/>

2. Science Objectives

Our main science objective was to map the Amazon River basin twice at high resolution in order to determine the extent of inundation that occurs between the approximate low and high flood stage of the main stem of the Amazon River. The following actions were necessary to accomplish this goal:

First, obtain coast to coast imagery of Northern South America, in particular, of the Amazon river basin. Due to the timing of the activities of the JERS-1 SAR, this first mapping was obtained at the low flood of the main stem of the Amazon river. This baseline image was required in order to establish low flood characteristics such as minimum extent of open water, and areas flooded a majority of the year; and establish land cover (forest, non-forest, water, flooded forest) as measurable by L-band SAR for a continental scale region.

Second, obtain another coast-to-coast image acquisition at the high flood of the main stem of the Amazon River. This data would establish the approximate maximum extent of flooding, the approximate maximum area of open water, and, together with the low flood data, determine the difference in flooding extent (both open water and forest area) between the approximate low and high flood of the Amazon river and its tributaries.

Third, mosaic the imagery into regional geolocated data sets, such that the high and low flood data could be easily compared pixel by pixel for differences in SAR backscatter. This step required that the data be well-calibrated radiometrically, and that the geolocation accuracy be well known in order to facilitate validation. (Siqueria, et al, 2000)

Fourth, validation of the inundation extent as measured by the JERS-1 SAR imagery had to be performed in order to legitimize the result. A description of this activity may be found in Hess et al (this issue).

Our secondary science objective was to determine how well simple land cover types might be classified from large regional SAR data sets. This was accomplished concurrently with our primary objective to map inundation. The exploration of the rich JERS-1 data source followed a three stage succession:

First, generate from the high-resolution data sets lower resolution backscatter and texture imagery. These products are described more fully in section 4.

Second, allow open access by science investigators to the observed, uninterpreted data products to encourage experimentation with a variety classification schemes. For example, see: Saatchi, et al (2000), and Podest and Saatchi (this issue).

Third, perform experimentation on the separability of classes and classification schemes. In particular, to verify that the data products are well calibrated enough for classification analysis.

3. PRE-GRFM CAMPAIGNS

As a first step towards using JERS-1 SAR data to map the vegetation cover over the entire Amazon basin, we conducted a precursor campaign in 1993 in the Western Amazon at the Manu National Park in Peru. The campaign involved ground measurements and near simultaneous overflights of JERS-1 and the NASA/JPL Airborne Synthetic Aperture Radar (AIRSAR) systems. One objective of the campaign was to see if JERS-1 SAR image data alone could be used to classify different vegetation cover types in this remote, relatively undisturbed region of the Amazon basin.

On June 7, 1993, AIRSAR underflew JERS-1 near Manu National Park. The three frequency (C-band, L-band, and P-band), fully polarimetric system (Lou, et al, 1996) imaged roughly the same area as that imaged by JERS-1 on the same date. See figure 1 for a comparison of some of the imagery obtained. This data set, along with a JERS-1 image of the same area in October, 1992 and March, 1993, and a sequence of images near Manaus, Brazil, established the JAMMS observation strategy (Chapman, et al, this issue), the post-processing that would be required, and the necessity for mosaicking.

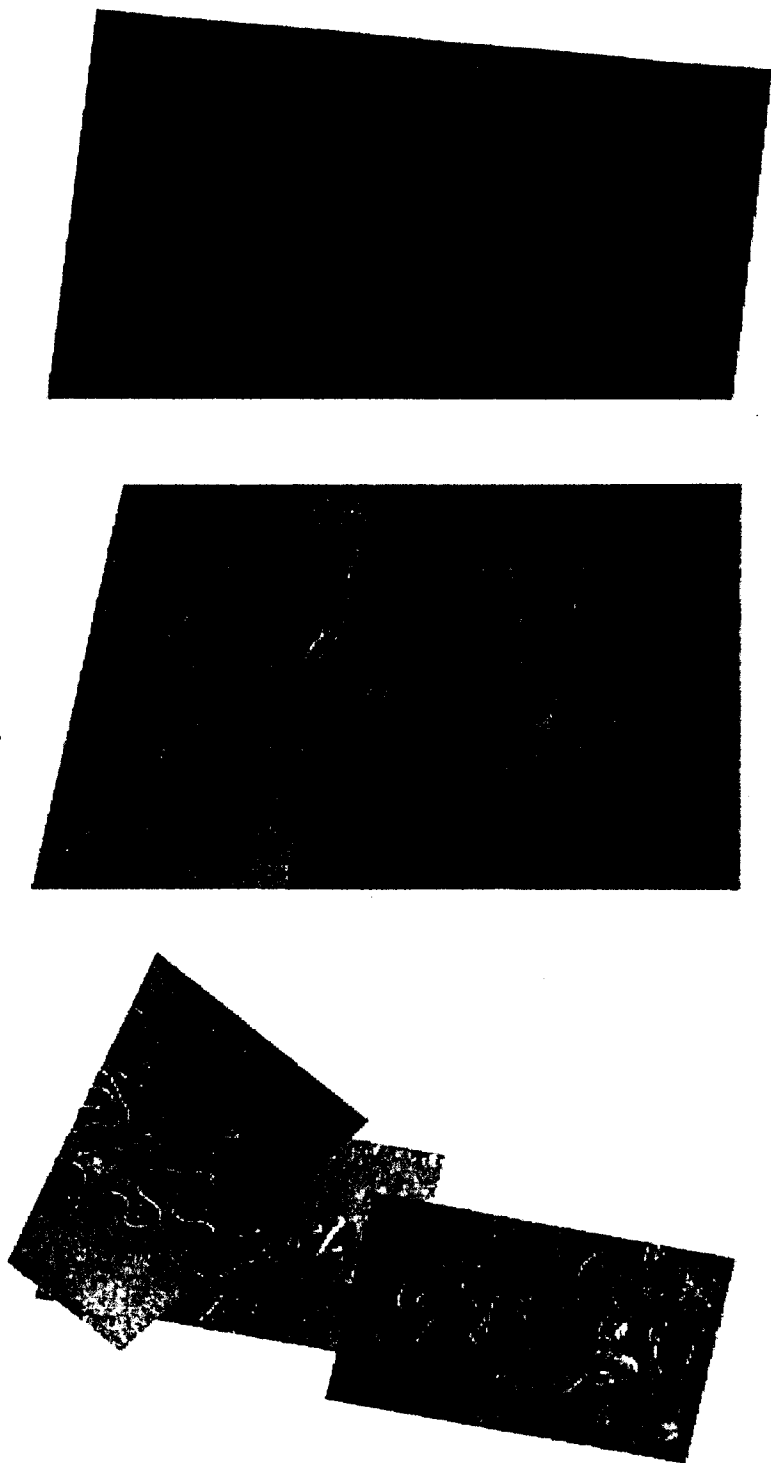


Figure 1: Subset of JERS -1 and AIRSAR imagery of Manu National Park, where the Rio Alto Madre de Dios and Rio Manu join to form the Rio Madre de Dios. A) Portion of JERS-1 SAR image. B) portion of AirSAR L-III mosaic. C) portion of three frequency AirSAR mosaic (Blue : Chh; Green : Lhh, Red : Phh).

A plant and wildlife preserve protecting areas of the Western Amazon, Manu National park is a popular study site due to its biodiversity and pristine conditions. Three rivers dominate the area : the Rio Alto Madre de Dios and Rio Manu join to form the Rio Madre de Dios. This region experiences two seasons: the dry season lasting roughly from May to September and the wet season spanning October to April.

The imagery from this area, both AIRSAR and JERS-1 SAR, were initially analyzed to determine separability of land cover types, and resulted in the JAMMS processing architecture that was used to process the coast-to-coast data set. As such, the description of the land cover (Forest - hill, floodplain, and upland; low vegetation; water) that were used to determine our initial classification and image product assessments and definitions follow:

Several different forest types exist throughout the Western Amazon. Hill forests occur in hilly regions of Manu National Park north of the Rio Madre de Dios. The hills are from 20-30m high and between 50-150m wide, thereby protecting much of the forest from river flooding. Hill forest is composed of a mosaic of mature forests with a height ranging from 20-45m. On the hilltops the canopy is closed, while on the slopes and in rivulets between hills palm and bamboo becomes more prevalent. This forest type is also semi-deciduous, which implies that some tree species lose their leaves in the dry season. Due to the remoteness of much of the hill forest, it is the least studied forest type.

The upland forest is found between the base of the Andes and the Rio Manu. It is similar to the hill forest, but contains different soil and trees only 20-30m high. The canopy is uneven and much of the upland forest is deciduous, implying that this forest type should experience the greatest amount of leaf loss in the dry season.

The final forest type is the flood plain forest surrounding the rivers. Regular flooding damage occurs here, and therefore, many stages of forest succession can be found. For example, areas far from the rivers and flooding are the most mature, with a very homogeneous, closed canopy and an average height of 50m. The understory of this mature forest contains a homogenous growth of palms. As one approaches the rivers, however, a less regular forest can be found. Stands of almost pure *Heliconia* banana plants from 2-3m high signal the first stage of regrowth. In areas where severe flooding has killed everything, the forest is very disturbed with a dense cover of *liana* vines. These areas generate a strong L-band response due to a specular reflection from the trunk-ground interaction. Other areas known as Aguajales are characterized by stands of *Mauritia* palms. These palm stands range from very wet to dry and also generate a strong L-band response.

As the rivers meander through the Amazon, erosion and deposition create numerous sandbars and oxbow lakes, known as cochas. In time, these areas dry out and forest succession begins. The first stage beyond the sandbar or bare earth is grass. Next, brushy plants known as *Tessaria* begin to grow which are from 0.5-1.5m tall. Following *Tessaria* are two possible types of dominant land cover: either a 10-12m tall forest will grow, or caña brava plants, which resemble sugar cane, will fill-in. Finally, the last stage of succession is a forest ranging from 12-50m tall, commonly containing *cecropia* trees. In an initial classification scheme, areas denoted as low vegetation were patterned after vegetation in early successional stages found along the rivers or in old cochas.

4. JAMMS Data Processing

The JAMMS data processing had several requirements. First, we had to be able to absorb a large quantity of full resolution data from both NASDA and ASF (approximately 200 Gbytes, an enormous

quantity by 1995 standards). Therefore, one objective was to reduce the data volume by producing low-resolution products (and archive the full resolution products), and to put all products whether from ASF or NASDA into a common image format. Second, based on preliminary work, we wanted to produce a statistical spatial component of the imagery to assist in the ability to classify various land cover types. This “texture” measurement additionally allowed us to extract more information about the characteristics of the full resolution data in a low resolution and low data volume product. Thirdly, we had to iterate through the calibration process as we learned more thoroughly through the mosaicking process the radiometric characteristics of the data.

Through initial work prior to the start of the JAMMS task, it was found that mean backscatter and the standard deviation of texture (Swain, 1978) were useful as features for classification. While other texture measures are possible (for instance, Podest et al, this issue), this one based on the spatial statistics of the radar observations was judged sufficient for our simple classification objectives.

Figure 2 below shows the mean backscatter for a portion of one of the JERS-1 SAR images used in this study. The standard deviation of texture was calculated via the following formula:

$$\sigma_T^2 = \frac{N(\sigma_p/\mu_p)^2 - 1}{N + 1} \left(1 + \frac{1}{\text{SNR}} \right)^2$$

Where σ_p is the standard deviation of the pixel intensities over some area and μ_p is the mean pixel intensity. This texture measure is natural to radar images and is related to the proportion of dominant to background targets within the reduced resolution pixel. An example of a texture image is shown in Figure 3. During the 8x8 averaging down of the full-resolution JERS-1 SAR images, backscatter and texture images were created.

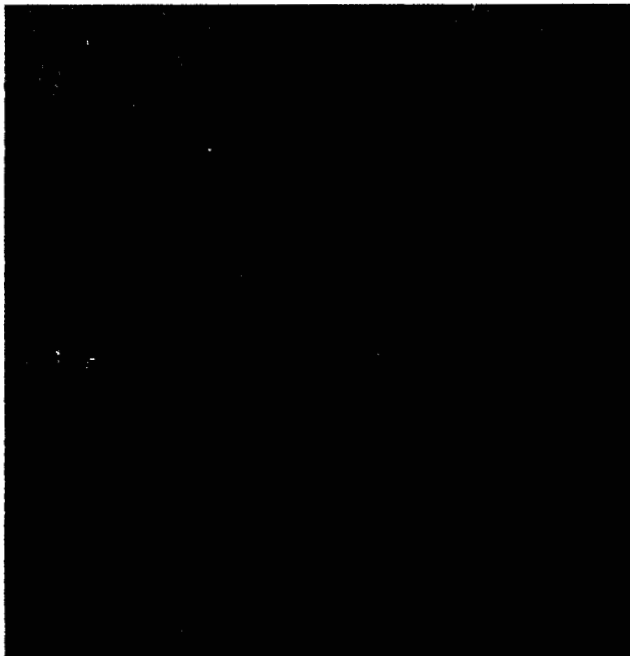


Figure 2: Low resolution (8x8 averaging) SAR backscatter image



Figure 3: Texture Map corresponding to Figure 2.

Texture was found to be a useful measurement in our advance work in the separability of land cover classes because it i.) helped distinctly separated the three forest classes, ii.) highlighted rivers hard to distinguish from backscatter alone, and iii.) was unaffected by first-order calibration errors. Using ground information from field campaigns in Peru (see previous section) and Brazil, texture and backscatter imagery for different land cover conditions were carefully scrutinized. In the next section, a full description of characteristic values is presented.

After data reduction, the low-resolution byte images from the low-flood (and high-flood) season were mosaicked together both at JPL (see Siqueira et al, 2000) and at NASDA using two different approaches. In addition to the geometric co-registration of the imagery, the calibration accuracy required far exceeded the pre-flight planned capabilities of the instrument. For a description of how a sufficiently high level of calibration accuracy was accomplished, please refer to Chapman, et al (this issue).

5. Classification methods

Unlike the classification of imagery from optical sensors, which are primarily based upon the color and ratio of colors of an object at perhaps a variety of bands in the optical and near optical portion of the spectrum, side-looking radar image classification is strongly dependent upon the structural components of natural and man-made elements in the illuminated ground swath. For example, at the L-band wavelength of the JERS-1 SAR, the brightest areas are generally the result of “double bounce” scattering, in which the signal travels from the satellite to the ground, to a component of the tree trunk, and back to the radar while experiencing only a minor loss of power in each scattering event. Compare this to specular scattering along, where a signal reflects off of a smooth surface, thus scattering the majority of the energy into the

forward direction and not back to the radar. Thus, double bounce reflections are significantly brighter than water or open terrain type reflections.

It has been found through analysis of the JERS-1, AirSAR and SIR-C data that flooded forests have high backscatter due to “double bounce” scattering (Hess et al, 1995), that water and low vegetation have low backscatter due to specular reflection away from the illuminating source and forests have intermediate backscatter due to diffuse scattering from the forest canopy (Durden et al, 1991). The range of backscatters that make up the overall mosaic depend on a mixture of these scattering mechanisms and other effects relating to topography, moisture and landcover type.

For the case of JERS-1, only one polarization channel is available (HH), which makes the measure of backscatter power alone insufficient for differentiating between some fundamental terrain and land cover types of interest. However, while the image texture does not reveal anything about the scattering mechanisms involved, we have found that it can help distinguish areas that have similar scattering mechanisms, but resulting from different targets and patterns of targets on the ground.

Problem areas for the L-band JERS-1 SAR are differentiating between open water and low vegetation areas (due to the low signal to noise ratio of this instrument), separating flooded forests from urban areas (which also exhibit double bounce returns), and differentiating floating grasses (called macrophytes) from the surrounding water and vegetation.

In addition, problems specific to this task include radiometric calibration errors (even those well within the designed specification for the JERS-1 SAR), the time lag between the beginning and end of data acquisitions (in which seasonal change can have a profound impact on the imagery), and replacement data takes from different epochs when an acquisition failed.

In the remainder of this discussion, we will examine a specific classification technique. In particular, a simple classification technique based upon backscatter and image texture values will be described.

Maximum-likelihood Classification

The classification scheme described in detail here is based on a supervised, Bayesian, maximum-likelihood classifier. Essential components of such a classifier are the following:

- (1) A feature vector containing the measurements of interest is identified
- (2) Training patterns representing distinct classes
- (3) Statistical models of these classes
- (4) Decision rules to determine which class the feature vector is most likely to belong

We used a feature vector comprised of two components: estimated backscatter (σ^0), and the texture measurement discussed earlier. Each pixel in a JERS-1 image to be classified is represented by these two measurements.

The June 7, 1993 image from Manu National Park in Peru provided all of the training data for the classifier, and will be referred to as the training image. From comparison of this scene to ground measurements, six vegetation classes could be distinguished. These classes are as follows:

- (1) Highly textured forest represented by hill forest
- (2) Medium textured forest represented by flood plain forest
- (3) Low textured forest represented by forest on a smooth plateau unaffected by flooding
- (4) Palm stands and areas with a bright L-band response
- (5) Low vegetation such as Boca Manu airstrip and drained cochas
- (6) Open water

Once these classes were chosen, training patterns were created to provide a model of each class. These are illustrated below:

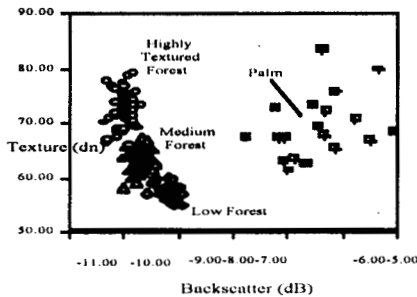


Figure 4: Training Patterns Created by Averaging Over 15x15 Boxes

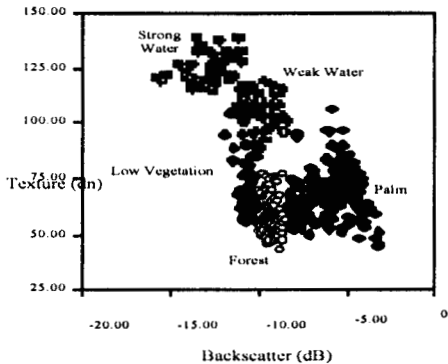


Figure 5: Training Patterns Created by Averaging Over 3x3 Boxes

Next the mean, variance, and covariance of both σ^0 and texture were calculated for each class. A masking approach was taken to remove those areas corresponding to open water from the classification process. This involved convolution with an edge-detecting filter, followed by thresholding and then region growing to find the paths followed by the rivers within the scene. Figure 6 shows an example of such a mask. Masking of open water was desirable, due to the similarity of backscatter values of open water and low vegetation areas.



Figure 6: Mask for water areas

Preliminary Classification

Before classifying a JERS-1 image, the image must first be calibrated (Shimada 1993). However, some residual calibration errors may remain which can cause the classifier to break down. Cross-track calibration errors, for example, appear as dark or bright vertical bands throughout an image, resulting in unclassified or misclassified forests. Therefore, before an image was classified it was corrected with respect to the original training image.

Since the texture measurement is essentially a ratio of standard deviation over mean, first-order calibration errors, such as radiometric offsets or linear trends, cancel, having no effect on the texture. The most significant error source for the texture measure is the SNR estimate. Therefore, the texture image corresponding to each backscatter image was left untouched and was assumed to be correct.

The accuracy of the classifier was evaluated by comparing the areas used to create the training patterns with the results of the final classification. Since the training patterns were created by averaging over 3x3 and 15x15 boxes of pixels, a representative pixel from each box was compared to the corresponding pixel in the final classification. In Table 1, the Percent column consists of the representative pixels matching the final classification divided by the total number of 3x3 and 15x15 boxes used to create the training pattern.

Class	Percent
Highly Txr. Forest	88%
Medium Txr. Forest	66%
Low Txr. Forest	90%
Palm	91.2%
Low Vegetation	48%

Water	93.4%
-------	-------

TABLE 1. *Classifier Accuracy*

This classification was then applied to the entire dry season mosaic as illustrated in figure 7. The main value of this result was to confirm that the data set was sufficiently well calibrated to allow a single algorithm to be applied across it and also to identify areas where ambiguous signatures may be a problem in future classification efforts, for example, in trying to separate very low vegetation savannas from open water.

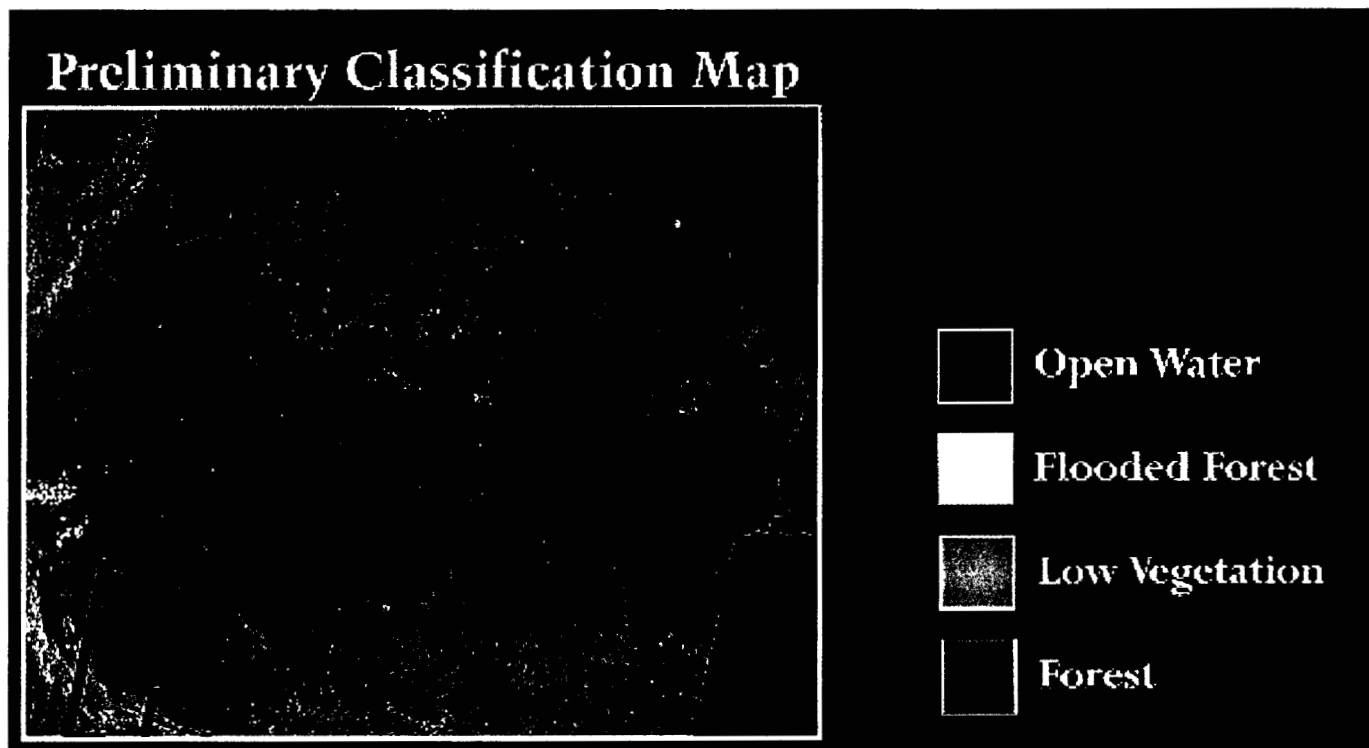


Figure 7: Simple Maximum likelihood classification of dry season mosaic.

The next step was to take a look at an entire sequence of classifications of an image set. In two image sequences (a color composite is shown in figure 8), areas of bright L-band response were seen to shrink and grow as the seasons change. This effect was attributed to the result of flooding or sensitive palms growing or losing leaves in response to water.

With both dry season and wet season data the feature space becomes much richer. It is straightforward to generate mean and texture data sets for each observation date, and the ratio between the mean values is also of interest due to its normalized sensitivity to change. The added dimension this gives to the data set is illustrated in Figure 8a. With more features available it is possible to separate more land cover classes in the data. This is demonstrated in Figure 8b, which shows the results of applying a supervised maximum likelihood classifier to the multi-season data. Here six classes are separable with reasonable success.



Figure 8 a: 2-season composite image of an area southwest of Manaus, Brazil with red as the flooded season backscatter, green as the dry season backscatter, and blue representing the ratio between the two.

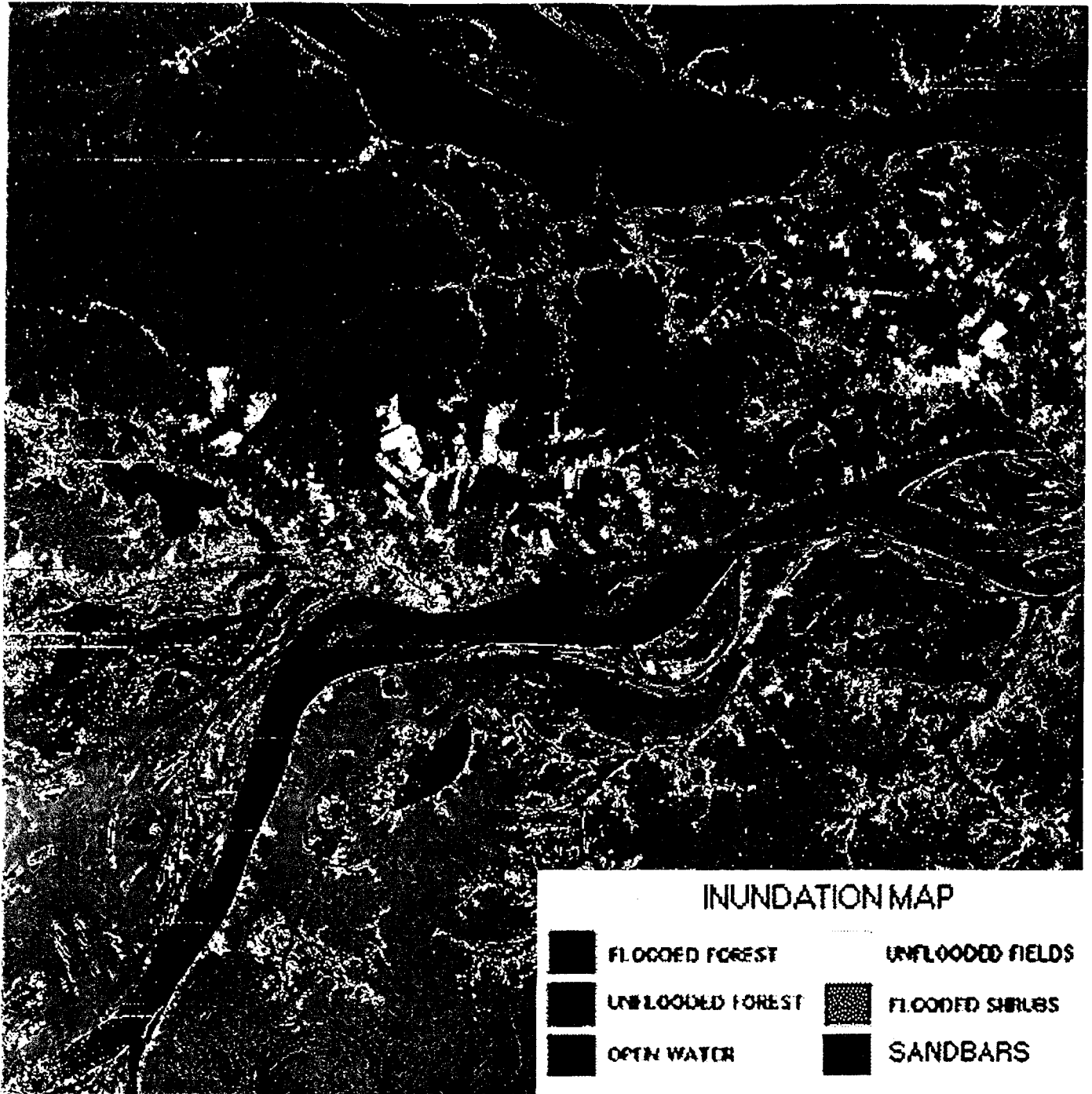


Figure 8b: Example resulting supervised classification for an area southwest of Manaus, Brazil

To further illustrate this point, Table 2 shows classification accuracies for the single-season data used separately, and the significant improvement obtained when the combined high-flood and low-flood data are used.

Class	High + Low Flood	High Flood only	Low Flood only
Water	99.2	53.9	97.4

Forest	93.2	64.7	61.6
Flooded Forest	96.4	96.8	50.2
Flooded Shrub	66	18	40
Clear Cut	80.6	50	22.2
Clear Cut 2	86.4	74.2	74.2
Sandbar	77.9	57.9	18.6
Total	92.2	65.9	63.8

Table 2: Classification accuracies for supervised classification of multi-season JAMMS data for the area shown in Figure 8.

The work for incorporating the entirety of the low and high flood mosaics is ongoing.

6. Implications for Future Missions

Resulting from the GRFM project were a number of advancements relating to SAR imaging and the characterization of rainforests that will have implications for future efforts in landcover monitoring and mission designs.

The first and most obvious of these is the utility of initiating large-scale mapping campaigns that have both a detailed science plan and generalized observing strategy for providing data products for applications not yet conceived. The need for a map of flooding inundation gave the leading justification which led to two-season “snapshot” coverage over the entire extent of the Amazon rainforest. The result were two high-resolution continental-scale images of interest and use to a large and diverse community, extending from students, scientists and environmentalists studying the region, to oil companies and government entities whose intent is to inventory resources and plan their environmentally safe and conscientious development. In all cases, the extensive images obtained promote awareness of the region and provide a benchmark for monitoring future change.

Programatically, the GRFM provided unique opportunities for international collaboration on data processing and analysis resulting in a combined effort whose results were greater than the sum of its parts. This synergy occurred by way of scientists from multiple organizations working toward the same goal by breaking it into similar yet unique manageable parts. Hence, methods for mosaicking, calibrating and classifying the data were individually developed within the various centers and the results compared and discussed at yearly workshop meetings. The information and techniques garnered from the workshops were taken back to their home institutions to improve processing methods and to advance the research in preparation for the next meeting.

JPL collaboration with researchers from the Institute for Computational Earth System Science (ICESS) at the University of California, Santa Barbara (UCSB), provided interaction and feedback with researchers actively studying field sites within the regions being imaged. Not only was this instrumental in the interpretation of the collected imagery, but it guided the development of the two-season data set into a user tested and validated resource. The geographical expertise of UCSB fed back into the geographic accuracy of the data set by providing comparison between the developed mosaics and known points on the ground derived from maps or specific locations in field test sites. For the given set of inputs, the resulting mosaic thus was tested and corrected to achieve the best achievable accuracy, be it geometric, radiometric or thematic.

Finally, a new method for obtaining wide-region coverage over relatively short time scales was developed and demonstrated through the GRFM. As with many instruments, there is often a tradeoff between complexity in the design vs. the degree of post-processing necessary to execute a desired task.. In the case of SAR, a somewhat complicated observing strategy called scansar is often implemented to extend the cross-track swath by electronically steering the antenna beam both in azimuth and elevation. The tradeoff for implementing scansar can be noticed in a slight loss in radiometric quality of the data because of the large range of incidence angles and because of the potential for the antenna pattern to change as it is being steered. The advantage of scansar is that the wide-swath image is obtained within the brief period that the satellite passes over the target region (less than one minute), and thus, this mode is often of use in oceanography for studying currents, etc. For many terrestrial applications however, the time-scale of change is on the order of days if not weeks; hence a steady progression of passes over a region can be stitched together, with the result being just as effective and useful (if not more so) as scansar. The result of implementing this observing strategy is to allow simplification in instrument design and data processing.

ACKNOWLEDGMENTS

The research described in this paper was carried out by the Jet Propulsion Laboratory, California Institute of Technology, under a contract with the National Aeronautics and Space Administration. The authors wish to thank Earth Observation Research Center of the National Space Development Agency of Japan for establishing the Global Rain forest Mapping Project, and, in particular, we thank Ake Rosenqvist and Masanobu Shimada. We also thank the Alaska SAR Facility for processing the most of the data from South and Central America. We thank Diane Wickland of NASA for supporting this task. We also thank Erika Podest, Laura Hess, Marcos Alves, John Holt, Christopher Kramer, Victor Taylor, Reiner Zimmermann, Verne Kaupp, and Greg McGarragh. For our participation in the NASA HPCC CAN, we also thank Dave Curkendall, Herb Siegel, and Craig Miller. We also thank our collaborators at JRC (In particular : Frank DeGrandi, Ake Rosenqvist, and Yryo Rauste) INPA (Bruce Forsberg) and INPE (In particular : Luciano Dutra).

For further information on the Global Rain Forest Mapping project or on JERS-1 mapping of the Amazon, please visit our web site at URL: <http://trfic.jpl.nasa.gov/>

REFERENCES

- Durden, S., A. Freeman, J. Klein, G. Vane, H. Zebker, R. Zimmermann, and R. Oren, 1991, "Polarimetric radar measurements of a tropical rainforest", Proc of 3rd AIRSAR Workshop, JPL Pub 91-30, pp 205-210.
- Freeman, A., and Durden, S., 1998, "A three component scattering model for polarimetric SAR data", IEEE Trans. Geoscience Rem. Sensing, Vol 36, No. 3, pp 963-973.
- FREEMAN, A, CHAPMAN, B., AND ALVES, M.,1996, The JERS-1 Amazon Multi-mission Mapping Study (JAMMS), Proc of 1996 Intl. Geosci. Rem. Sens., pp830-833, Lincoln, Nebraska, 1996.
- Freeman, A., Alves, M. and Williams, J. "Calibration Results for JERS-1 SAR Data produced by the Alaska SAR Facility", Proceedings IGARSS '93, pp. 965-967.
- Hara., Y. and Ono, M., "Analysis of JERS-1 SAR Imagery", Proceedings IGARSS '93, pp. 1191-1193.

- Hess, L., L., J. M. Melack, S. Filoso, and Y. Wang, 1995, "delineation of inundated area and vegetation along the Amazon floodplain with the SIR-C SAR", *IEEE Trans. Geosci. Remote Sensing*, Vol 33, NO. 4, pp 896-904.
- Lou, Y., Kim, Y., vanZyl, J., 1996, "The NASA/JPL Airborne Synthetic Aperture Radar System", *Summaries of the Sixth Annual Airborne Science Workshop, Vol. II, AIRSAR Workshop, Held March 4-8, 1996 at JPL, Pasadena, CA*, pp. 51-55.
- NASDA EARTH OBSERVATION CENTER, 1995, *JERS-1 SAR Data Users Handbook*, NASDA EORC, Tokyo, Japan.
- Podest, E., and Saatchi, S., 2000, "Application of Multi-scale Texture Features for Mapping Tropical Land Cover Types Using JERS-1 Radar Data", submitted to this issue.
- Rauste, Y., Richards, T., DeGrandi, G., Perna, G., Franchino, E. And Rosenqvist, Å, 1999, "Compilation and Validation of the GRFM Africa (SAR) Mosaics using Multi-temporal Block Adjustment, JERS-1 Science Program '99 PI reports, March 1999, EORC, NASDA, Japan.
- ROSENQVIST, AKE , 1996, The global rain forest mapping project by JERS-1 SAR , *Proc of XVIII ISPRS Cong. In Vienna, Austria, 1996*.
- Rosenqvist, Å, Shimada, M., Chapman, B., Freeman, A., DeGrandi, G., Saatchi, S., and Rauste, Y., 2000, "The Global Rain Forest Mapping Project - A Review", *Int. J. Rem. Sens.*, Vol. 21, No. 6 & 7, pp. 1375-1387.
- Saatchi, S., Nelson, B., Podest, E., and Holt, J., 2000, "Mapping Land Cover types in the Amazon Basin using 1km JERS-1 mosaic", *Int. J. Rem. Sens.*, Vol. 21, No. 6 & 7, pp. 1201-1234.
- Shimada, M., "JERS-1 SAR Calibration and Validation", presented at the CEOS SAR Calibration Workshop, Noordwijk, The Netherlands, September 1993.
- SIQUIERA, P., HENSLEY, S., SHAFFER, S., HESS, L., MCGARRAGH, G., CHAPMAN, B., HOLT, J., AND FREEMAN, A., 2000, A continental scale mosaic of the Amazon basin using JERS-1 SAR, accepted, *IEEE Transactions Geoscience and Remote Sensing*.
- Siqueira, P., Hensley, S., Shaffer, S., Hess, L., McGarragh, G., Chapman, B., Holt, J., and Freeman, A., 2000, "A continental Scale Mosaic of th Amazon Basin using JERS-1 SAR", accepted, *IEEE transactions Geoscience and Remote Sensing*.
- Simard, Marc, Saatchi, Sasan, and DeGrandi, Gianfranco, 2000, " The use of Decision Tree and Multi-scale Texture for Classification of JERS-1 SAR Data over Tropical Forest, accepted *IEEE Geoscience and Remote Sensing, IGARSS99 special issue*.
- Swain P. H., *Remote Sensing, the Quantitative Approach*. United States of America: McGraw-Hill, Inc., 1978.
- Yamagata, Y. and Yasuoka, Y., "Classification of Wetland Vegetation by Texture Analysis Methods using ERS-1 and JERS-1 Images", *Proceedings IGARSS '93*, pp. 1614-1616.